AIP | The Journal of Chemical Physics

Communication: Multiple-property-based diabatization for open-shell van der Waals molecules

Tijs Karman, Ad van der Avoird, and Gerrit C. Groenenboom

Citation: The Journal of Chemical Physics **144**, 121101 (2016); doi: 10.1063/1.4944744
View online: http://dx.doi.org/10.1063/1.4944744
View Table of Contents: http://scitation.aip.org/content/aip/journal/jcp/144/12?ver=pdfcov
Published by the AIP Publishing

Communication: Multiple-property-based diabatization for open-shell van der Waals molecules

Tijs Karman, Ad van der Avoird, and Gerrit C. Groenenboom[a)]
Theoretical Chemistry, Institute for Molecules and Materials, Radboud University, Heyendaalseweg 135, 6525 AJ Nijmegen, The Netherlands

(Received 22 January 2016; accepted 13 March 2016; published online 24 March 2016)

We derive a new multiple-property-based diabatization algorithm. The transformation between adiabatic and diabatic representations is determined by requiring a set of properties in both representations to be related by a similarity transformation. This set of properties is determined in the adiabatic representation by rigorous electronic structure calculations. In the diabatic representation, the same properties are determined using model diabatic states defined as products of undistorted monomer wave functions. This diabatic model is generally applicable to van der Waals molecules in arbitrary electronic states. Application to locating seams of conical intersections and collisional transfer of electronic excitation energy is demonstrated for O_2–O_2 in low-lying excited states. Property-based diabatization for this test system included all components of the electric quadrupole tensor, orbital angular momentum, and spin-orbit coupling. © *2016 AIP Publishing LLC.* [http://dx.doi.org/10.1063/1.4944744]

I. INTRODUCTION

The Born-Oppenheimer approximation is at the heart of molecular physics,[1] leading to a two-stage treatment of electronic and nuclear degrees of freedom. The Born-Oppenheimer *adiabatic* approximation, neglecting nuclear-derivative couplings between electronic eigenstates,[2] breaks down for systems with close-lying electronic states.[3–5] Rather than explicitly including these couplings in dynamical calculations, it is often advantageous to use a *diabatic* representation in which the derivative couplings are negligible, at the cost of introducing off-diagonal terms in the electronic potential.[2,5,6]

This Communication considers diabatization for complexes containing open-shell or electronically excited molecules, where diabatization is necessary due to the presence of asymptotically degenerate states. For van der Waals molecules, diabatic states are defined as products of rotated monomer wave functions.[7] In the previous work on such systems, the transformation to this diabatic representation has been obtained by manual inspection of the electronic wave function,[7] or by considering only geometries for which the transformation is determined by symmetry.[8] Property-based diabatization is also possible,[4,9] for example, simply by diagonalizing the matrix representation of a property.[10] However, it is not always possible to distinguish multiple states using a single property,[9] and the diagonalization of a property matrix does not provide a phase definition.

In this Communication, we present a new method based on fitting a similarity transformation to a set of property matrices known in both representations. Any number of properties may be included on equal footing and the employed diabatic model provides a consistent phase definition of the diabatic states. The presented diabatic model is generally applicable to van der Waals molecules in arbitrary electronic states. As a test system, we consider the low-lying electronic states of O_2–O_2 correlating to monomers in the $X^3\Sigma_g^-$, $a^1\Delta_g$, and $b^1\Sigma_g^+$ states. Due to the long life-time of the singlet excited states, the collision dynamics in this system is of importance for atmospheric excitation energy transport,[11,12] and the related collision-induced absorption spectra are of interest for calibration of remote-sensing missions.[13]

II. PROPERTY-BASED DIABATIZATION ALGORITHM

The proposed algorithm consists of the following three steps:

1. A number of properties are calculated in the adiabatic representation, that is, in the space of eigenfunctions of the electronic Hamiltonian. We denote the $n \times n$ matrix representations of these properties in the adiabatic basis by $\boldsymbol{A}_p$, where p enumerates different properties and n is the number of states. These properties can be evaluated using any electronic structure program, at a computational cost negligible compared to that of calculating the electronic eigenstates.
2. We denote the $n \times n$ matrix representations of these same properties in the diabatic basis by $\boldsymbol{D}_p$. These are obtained from a diabatic model that employs products of undistorted monomer wave functions as diabatic states. This allows to calculate the matrices $\boldsymbol{D}_p$ in terms of monomer properties, as is explained in more detail in Sec. III.
3. In the last step, we fit a unitary transformation, $\boldsymbol{U}$, that best maps the set of matrices $\boldsymbol{A}_p$ onto the set $\boldsymbol{D}_p$. This transformation gives the relation between adiabatic and diabatic states, and can be used to transform the potential energy, or other *ab initio* computed properties, to the

a)Electronic mail: gerritg@theochem.ru.nl

diabatic representation as $\boldsymbol{V}^{(\text{diabatic})} = \boldsymbol{U}\boldsymbol{V}^{(\text{adiabatic})}\boldsymbol{U}^{\dagger}$. The algorithm that determines this transformation is described next.

We are looking for a unitary transformation $\boldsymbol{U}$ that transforms between the diabatic and adiabatic representations, and hence satisfies

$$\boldsymbol{U}\boldsymbol{A}_p\boldsymbol{U}^{\dagger} = \boldsymbol{D}_p \qquad \forall \text{ properties } p. \tag{1}$$

In general, this equation cannot be satisfied exactly due to discrepancies between the rigorous electronic structure calculations in which $\boldsymbol{A}_p$ are determined and the simple model that yields $\boldsymbol{D}_p$. Instead, we therefore minimize the square Frobenius norm of the residual, summed over all properties p with weight w_p,

$$\begin{aligned}\sum_p w_p \|\boldsymbol{U}\boldsymbol{A}_p - \boldsymbol{D}_p\boldsymbol{U}\|^2 &= \sum_p w_p \text{Tr}\left[\left(\boldsymbol{U}\boldsymbol{A}_p - \boldsymbol{D}_p\boldsymbol{U}\right)^{\dagger}\left(\boldsymbol{U}\boldsymbol{A}_p - \boldsymbol{D}_p\boldsymbol{U}\right)\right] \\ &= \sum_p w_p \text{vec}(\boldsymbol{U})^{\dagger}\boldsymbol{M}_p^{\dagger}\boldsymbol{M}_p \text{vec}\,(\boldsymbol{U})\,.\end{aligned} \tag{2}$$

In the last step, we introduced the vectorization of $\boldsymbol{U}$, denoted by vec $(\boldsymbol{U})$, which maps an $n \times n$ matrix onto a n^2 dimensional vector by stacking its columns. The $n^2 \times n^2$ matrix $\boldsymbol{M}_p$ is given by

$$\boldsymbol{M}_p = \boldsymbol{A}_p^T \otimes \mathbf{1} - \mathbf{1} \otimes \boldsymbol{D}_p, \tag{3}$$

with $\mathbf{1}$ the $n \times n$ identity matrix.

To obtain non-trivial solutions that minimize Eq. (2), we introduce the constraint $\text{vec}(\boldsymbol{U})^{\dagger}\text{vec}\,(\boldsymbol{U}) = 1$ using the Lagrange undetermined multiplier method. This yields the eigenvalue equation

$$\left[\sum_p w_p \boldsymbol{M}_p^{\dagger}\boldsymbol{M}_p\right] \text{vec}\,(\boldsymbol{U}) = \lambda \text{vec}\,(\boldsymbol{U})\,. \tag{4}$$

This eigenvalue equation can be solved using standard numerical methods, and the matrix $\boldsymbol{U}$ is obtained by appropriately reshaping the eigenvector corresponding to the lowest eigenvalue. However, as long as the eigenvalue zero is degenerate, the solution of Eq. (4) is not unique. This issue is resolved by adding more properties, which can only increase the obtained eigenvalues since each term, $\boldsymbol{M}_p^{\dagger}\boldsymbol{M}_p$, is positive semi-definite. Therefore, the degeneracy of an eigenvalue zero may be lifted by including the appropriate properties in the analysis. Finally, we note that the solution to Eq. (4) can be determined up to an overall phase of all states, which does not affect any properties transformed using Eq. (1). The relative phases of the adiabatic states, the columns of $\boldsymbol{U}$, are determined completely by the unique solution to Eq. (4). This phase information is required for transforming *ab initio* transition moments to the diabatic representation.

The imposed constraint does not guarantee unitarity of the matrix $\boldsymbol{U}$. However, if the transformation between the adiabatic and diabatic representations is uniquely determined, the matrix $\boldsymbol{U}$ should be close to unitary, unless the diabatic model used to obtain $\boldsymbol{D}_p$ was inaccurate. The nearest exactly unitary matrix is then found using a singular value decomposition,

$$\boldsymbol{U} = \boldsymbol{L}\boldsymbol{\Sigma}\boldsymbol{R}^{\dagger}, \tag{5}$$

where $\boldsymbol{L}$ and $\boldsymbol{R}$ are unitary matrices whose columns contain the left and right singular vectors, respectively, and $\boldsymbol{\Sigma}$ is a diagonal matrix whose non-negative diagonal elements are the singular values. Setting the singular values to unity gives the nearest unitary matrix

$$\boldsymbol{U}' = \boldsymbol{L}\boldsymbol{R}^{\dagger}. \tag{6}$$

III. DIABATIC MODEL FOR VAN DER WAALS MOLECULES

For van der Waals molecules, quasi-diabatic states can be defined as products of rotated undistorted monomer states

$$|\psi_A\psi_B\rangle = \left[\hat{\mathcal{R}}(\Omega_A)|\psi_A\rangle\right] \otimes \left[\hat{\mathcal{R}}(\Omega_B)|\psi_B\rangle\right], \tag{7}$$

where $|\psi_A\rangle, |\psi_B\rangle$ are monomer electronic states, defined in a monomer-centered frame, and $\hat{\mathcal{R}}(\Omega_X)$ is a rotation operator depending on the Euler angles of molecule X. Neglecting intermolecular exchange, we have suppressed the formal antisymmetrization of the electronic states. We now consider one-electron properties which are written as direct sums of the monomer one-electron property

$$\hat{O} = \hat{O}^{(A)} \otimes \hat{1}^{(B)} + \hat{1}^{(A)} \otimes \hat{O}^{(B)}. \tag{8}$$

For the dimer, we find the following matrix element in the diabatic representation:

$$\begin{aligned}\langle\psi_A\psi_B|\hat{O}|\psi'_A\psi'_B\rangle &= \delta_{\psi_A,\psi'_A}\langle\psi_B|\hat{\mathcal{R}}(\Omega_B)^{\dagger}\hat{O}^{(B)}\hat{\mathcal{R}}(\Omega_B)|\psi'_B\rangle \\ &\quad + \langle\psi_A|\hat{\mathcal{R}}(\Omega_A)^{\dagger}\hat{O}^{(A)}\hat{\mathcal{R}}(\Omega_A)|\psi'_A\rangle\delta_{\psi_B,\psi'_B}.\end{aligned} \tag{9}$$

If the one-electron property is the q-th component of a rank-k spherical tensor, denoted as $\hat{O}_q^{(k)}$, we find for the monomer matrix element

$$\langle\psi_X|\hat{\mathcal{R}}^{\dagger}\hat{O}_q^{(k)}\hat{\mathcal{R}}|\psi'_X\rangle = \sum_{q'}\langle\psi_X|\hat{O}_{q'}^{(k)}|\psi'_X\rangle D_{q',q}^{(k)}(\hat{\mathcal{R}}^{-1}). \tag{10}$$

That is, under rotation, a spherical tensor operator transforms amongst its components with coefficients given by Wigner D-matrix elements.[14] The transition moments between the monomer states, $\langle\psi_X|\hat{O}_{q'}^{(k)}|\psi'_X\rangle$, are obtained in an electronic structure calculation for an isolated monomer $X = A, B$ in the monomer-centered frame. This calculation has to be performed only once, and defines a phase convention for the diabatic states.

For the low-lying electronic states of O_2–O_2 considered as a test system, $|\psi_A\rangle, |\psi_B\rangle \in |X^3\Sigma_g^-\rangle, |a^1\Delta_g\rangle, |b^1\Sigma_g^+\rangle$. The a and b excited monomer states lie 7918 cm^{-1} and 13 195 cm^{-1} above the ground state, respectively. This gives rise to ten singlet states, seven triplet states, and one quintet state. The different total electron spin states are not coupled by non-adiabatic couplings, and are therefore diabatized separately. The properties that we include are the orbital angular momentum and the electric quadrupole moment, which transform according to Eq. (10) as spherical tensors with rank $k = 1$ and $k = 2$, respectively. With properties in atomic units, we use equal weights $w_p = 1$ for all tensor components, and have not found it necessary to adjust these weights.

For the ten singlet states of the complex, the procedure outlined above uniquely determines the transformation between the diabatic and adiabatic representations. For the seven triplet states, we however encountered the following problem. Apart from the triplet ground state, which is energetically well-separated from the other states, all electronic states correlate to one monomer in the $X^3\Sigma_g^-$ ground state and the other in the $a^1\Delta_g$ or $b^1\Sigma_g^+$ excited states. Because the included properties do not couple the ground and excited monomer states, all matrices $\boldsymbol{D}_p$ are block-diagonal in the localization of the excitation, and the matrix $\sum_p w_p \boldsymbol{M}_p^\dagger \boldsymbol{M}_p$ will be block-diagonal as well. Both blocks have at least one eigenvalue close to zero, and the resulting transformation will not be unique. Fortunately, this does not lead to a continuum of possible transformations corresponding to arbitrary mixing of two degenerate eigenvectors, but after imposing unitarity, only two distinct possibilities remain. In order to uniquely determine this transformation, we also include spin-orbit coupling. We transform the spin-orbit coupling obtained in the monomer-based diabatic model to the adiabatic representation using both possible transformations, and compare the resulting adiabatic spin-orbit couplings to the results of *ab initio* calculations in order to uniquely determine the correct transformation.

IV. RESULTS

In this section, we show results for application of the reported diabatization algorithm to the low-lying triplet states of O_2–O_2, with the monomers in the electronic $X^3\Sigma_g^-$, $a^1\Delta_g$, and $b^1\Sigma_g^+$ states. All electronic structure calculations are performed using the internally contracted multi-reference configuration interaction method with Davidson's size-consistency correction (MRCISD+Q) in an aug-cc-pVTZ basis set, as implemented in the Molpro package.[15] Molecular orbitals and reference functions are calculated in state-averaged complete active space self-consistent field calculations, averaging over the subsets of nearly degenerate states that correlate to the same dissociation limit. The active space contains the 12 electrons in the 8 orbitals that correlate to the molecular π and π^* shells.

First, we confirm that the proposed algorithm uniquely defines the transformation between adiabatic and diabatic representations. The uniqueness of the transformation matrix is determined by the non-degeneracy of the lowest eigenvalue of the matrix $\sum_p w_p \boldsymbol{M}_p^\dagger \boldsymbol{M}_p$. To monitor this, we express the lowest eigenvalues in percent of the largest eigenvalue. Typically, the lowest two eigenvalues are on the order of 0.1%, whereas the third eigenvalue is much larger, typically around 15%. For parallel-displaced geometries, where $\Omega_A \approx \Omega_B$, the model has more difficulty to distinguish between the two molecules, resulting in somewhat larger and less well separated eigenvalues. As explained before, the correct transformation is determined uniquely by computing spin-orbit couplings between adiabatic states using both possible transformations. Typically, we find that one of the transformations reproduces the spin-orbit couplings to a few cm^{-1}, whereas the other is typically off by about 300 cm^{-1}, which uniquely establishes the former as the correct transformation.

As a simple test of the accuracy of the computed transformation and diabatic model, we compare adiabatic properties as calculated *ab initio* to those obtained by transforming the diabatic model to the adiabatic representation. We typically observe root-mean-square errors of few percent in the quadrupole tensor, half a percent in the spin-orbit coupling, and much less than one percent in the orbital angular momentum operator. The differences are largest for short separations and nearly collinear orientations of the O_2 monomers, and are due to the intermolecular interaction which is included in the MRCI calculations but not in the diabatic model.

Transformation to the diabatic basis smoothens the geometry dependence of all properties included in the analysis, as properties in the model are smooth by construction and the transformed diabatic model accurately reproduces the adiabatic properties. Other properties should also become smooth functions of the geometry. This is shown in Fig. 1 for the ϕ-dependence of the transition dipole moments connecting the triplet ground state to the lowest six excited states. These are interaction-induced dipole moments as the corresponding transitions violate both spin and spatial selection rules in the isolated monomers. Therefore, these properties cannot be

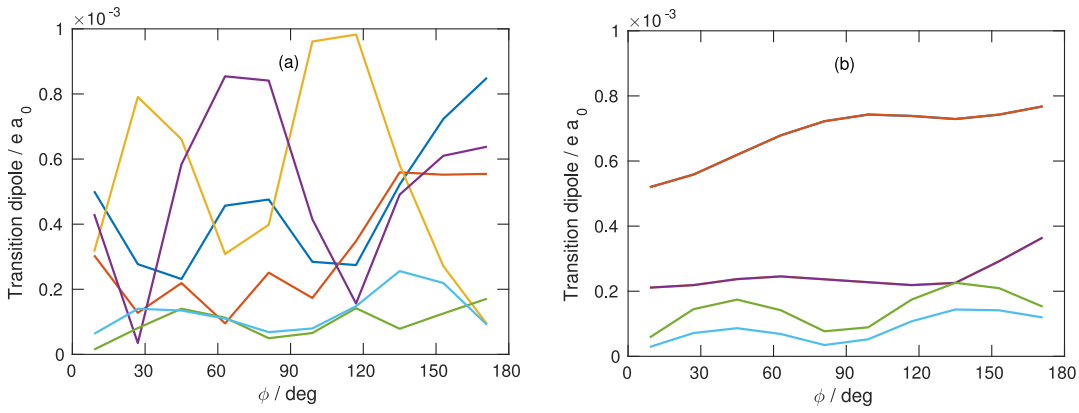

FIG. 1. Length of transition dipole moments connecting the triplet ground state with the six triplet excited states as a function of ϕ for fixed $\theta_A = 64.3°$, $\theta_B = 81.4°$, and $R = 5.75\ a_0$. Panels (a) and (b) show results in the adiabatic and diabatic representations, respectively.

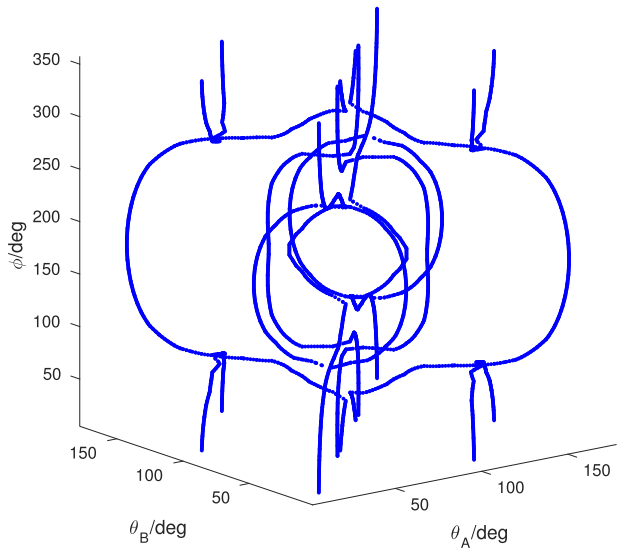

FIG. 2. The seam of conical intersections between the two states correlating to $O_2(X^3\Sigma_g^-)$–$O_2(b^1\Sigma_g^+)$ as a function of the Jacobi angles θ_A, θ_B, and ϕ at fixed $R = 7\ a_0$.

included in a diabatic model based on undistorted monomer wave functions, yet in the diabatic representation, they become smooth functions of the geometry.

Next, we test the accuracy of the diabatization algorithm for the high symmetry T-shaped geometry. In this case, each of the Cartesian-component diabatic states can be assigned to an irreducible representation of the C_{2v} point group, see the supplementary material.[16] Neglecting the mixing of energetically well-separated states, there should be one-to-one correspondence between the diabatic and adiabatic states, except for the two B_1 states correlating to $O_2(X^3\Sigma_g^-)$–$O_2(a^1\Delta_{xy})$, which can mix. By performing MRCI calculations, we verify that the correct symmetry-determined transformation is obtained to numerical precision also without explicitly including symmetry.

Figure 2 shows the seams of conical intersections for the two states correlating to $O_2(X^3\Sigma_g^-)$–$O_2(b^1\Sigma_g^+)$ at fixed $R = 7\ a_0$ as a function of the three angular coordinates. We locate the seam by first computing global diabatic potential energy surfaces, and interpolating the smooth diabatic potentials linearly between grid points. We locate the degeneracies of the two adiabatic energies as the roots of the discriminant of the characteristic polynomial of the 2×2 potential matrix.

Finally, we apply the diabatic potential energy surfaces[17] for the two states correlating to $O_2(X^3\Sigma_g^-)$–$O_2(b^1\Sigma_g^+)$ in order to compute cross sections for collisional transfer of the electronic excitation energy.[18] These cross sections are important for atmospheric excitation energy transport due to the long life-time of the oxygen singlet excited states.[11,12] We perform both fully quantum mechanical coupled-channel calculations and approximate semiclassical calculations.[16,19] In the semiclassical calculations, the translational degrees of freedom evolve according to the classical equations of motion for the isotropic potential, whereas all other degrees of freedom are treated quantum mechanically using the full

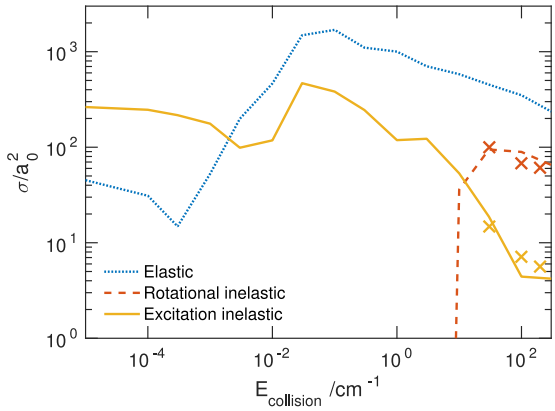

FIG. 3. Integral scattering cross sections for elastic, rotationally inelastic, and excitation inelastic transitions. Lines correspond to results of coupled-channels calculations, where symbols refer to approximate semiclassical calculations.

potential.[16,19] Figure 3 shows the resulting cross sections, where lines are obtained from coupled-channel calculations and crosses correspond to semiclassical results. Reasonable agreement between the approximate semiclassical and the full quantum results is obtained for high collision energies, and the energy dependence of the cross sections can be readily understood from the decreasing interaction time with increasing collision energy. For more details, the reader is referred to the supplementary material.[16]

V. CONCLUSIONS AND OUTLOOK

We have presented a method for determining the transformation between adiabatic and diabatic representations by requiring a set of properties in both representations to be related by a similarity transformation. Properties in the adiabatic representation can be computed with many electronic structure methods with negligible computational overhead. Diabatically, properties are obtained from a model based on undistorted monomer wave functions, which is generally applicable to van der Waals molecules.

We have demonstrated the stability of the diabatization algorithm for O_2–O_2 in low-lying electronic states. Where the transformation is determined by point-group symmetry, the correct transformation is recovered to numerical precision. We have also demonstrated application to locating seams of conical intersections and collisional transfer of electronic excitation energy. Providing a theoretical description of collision dynamics in these excited states and the related collision-induced absorption spectra constitutes our immediate work plan.

[1]M. Born and R. Oppenheimer, Ann. Phys. **389**, 457 (1927); Ann. Phys. IV **84**, 457 (1927).
[2]H. Köppel, W. Domcke, and L. S. Cederbaum, Adv. Chem. Phys. **57**, 59 (1984).
[3]D. R. Yarkony, J. Phys. Chem. A **105**, 6277 (2001).
[4]H. Nakamura and D. G. Truhlar, J. Chem. Phys. **115**, 10353 (2001).
[5]M. Baer, Phys. Rep. **358**, 75 (2002).
[6]C. A. Mead and D. G. Truhlar, J. Chem. Phys. **77**, 6090 (1982).
[7]P. E. S. Wormer, J. A. Kłos, G. C. Groenenboom, and A. van der Avoird, J. Chem. Phys. **122**, 244325 (2005).

[8]Q. Ma, J. A. Kłos, M. H. Alexander, A. van der Avoird, and P. J. Dagdigian, J. Chem. Phys. **141**, 174309 (2014).
[9]C. E. Hoyer, X. Xu, D. Ma, L. Gagliardi, and D. G. Truhlar, J. Chem. Phys. **141**, 114104 (2014).
[10]A. J. Dobbyn and P. J. Knowles, Mol. Phys. **91**, 1107 (1997).
[11]I. C. McDade and E. J. Llewellyn, Can. J. Phys. **64**, 1626 (1986).
[12]M. R. Torr and D. G. Torr, Rev. Geophys. Space Phys. **20**, 91, doi:10.1029/RG020i001p00091 (1982).
[13]C. Frankenberg, R. Pollock, R. A. M. Lee, J. Rosenberg-Blavier, D. Crisp, C. W. O'Dell, G. B. Osterman, C. Roehl, P. O. Wennberg, and D. Wunch, Atmos. Meas. Tech. Discuss. **7**, 7641 (2014).
[14]L. C. Biedenharn and J. D. Louck, *Angular Momentum in Quantum Physics*, Encyclopedia of Mathematics (Addison-Wesley, Reading, 1981), Vol. 8.
[15]MOLPRO is a package of *ab initio* programs written by H.-J. Werner and P. J. Knowles, with contributions from R. D. Amos, A. Berning, D. L. Cooper, M. J. O. Deegan, A. J. Dobbyn, F. Eckert, C. Hampel, T. Leininger, R. Lindh, A. W. Lloyd, W. Meyer, M. E. Mura, A. Nicklaß, P. Palmieri, K. Peterson, R. Pitzer, P. Pulay, G. Rauhut, M. Schütz, H. Stoll, A. J. Stone, and T. Thorsteinsson.
[16]See supplementary material at http://dx.doi.org/10.1063/1.4944744 for multiple-property-based diabatization for open-shell van der Waals molecules.
[17]T. Karman, A. van der Avoird, and G. C. Groenenboom, "Diabatic potential energy surfaces for the low-lying states of O_2–O_2" (unpublished).
[18]H. Massey, Contemp. Phys. **13**, 375 (1972).
[19]A. Semenov and D. Babikov, J. Phys. Chem. Lett. **5**, 275 (2014).